Appl. Phys. A (2016) 122:1073
DOI 10.1007/s00339-016-0602-x

Applied Physics A
Materials Science & Processing

Numerical study on the free vibration of carbon nanocones resting on elastic foundation using nonlocal shell model

Reza Ansari[1] · **Jalal Torabi**[1]

Received: 28 August 2016 / Accepted: 22 November 2016 / Published online: 3 December 2016

Abstract Employing the variational differential quadrature method, the free vibration of carbon nanocones (CNCs) embedded in an elastic foundation, is studied based on nonlocal elasticity theory. On the basis of the first-order shear deformation theory, the energy functional of the CNC is presented and then discretized by employing the generalized differential quadrature method in the axial direction and periodic differential operators in the circumferential direction. According to Hamilton's principle and using matrix relations, the reduced forms of mass and stiffness matrices are readily obtained. The results of present study are compared to those obtained by molecular mechanics to verify the proposed approach. In addition, the effects of nonlocal parameter, boundary conditions, semi-apex angle and both Winkler and Pasternak coefficients of elastic foundation are examined on the vibrational behavior of CNCs. The results indicate that the increase in nonlocal parameter and elastic foundation coefficients decreases and increases the fundamental frequency of CNCs, respectively.

1 Introduction

By the discovery of the carbon nanotubes, nanorods and nanocones, nanoscale engineering applications have received considerable attention. The high mechanical strength, low density and excellent thermal and electrical properties of nanomaterials make them suitable for various usages in micro-electro-mechanical systems (MEMS) and nano-electro-mechanical systems (NEMS). Ge and Sattler [1] discovered the carbon nanocones (CNCs) in 1994. Subsequently, the existence of only five apex angles of CNCs was verified by Krishnan et al. [2]. Due to the localization of electric field at sharp ends of CNCs, these nanostructures can be used as the high resolution probes in different systems such as atomic force microscopy and field emission devices [3, 4].

There are some experimental studies on the mechanical behavior of nanostructures [5–8]. Due to the difficulties of conducting the controlled experiments at nanoscale, the theoretical modeling is widely used to investigate the mechanical characteristics of nanostructures. There exist three main categories for the theoretical modeling of nanomaterials including atomistic modeling [9–13], hybrid atomistic-continuum mechanics [14, 15] and continuum modeling. For the large-scale nanostructures, the atomistic modelings such as molecular dynamics (MD) have a huge computational cost. However, the continuum mechanics provides a computationally efficient model which makes this category interesting for researchers.

Since at nanoscales the mechanical behavior of structures is size dependent [16, 17] and the classical continuum mechanics cannot capture the size effect, the modified continuum theories are needed. Among the size-dependent continuum theories, the nonlocal elasticity theory proposed by Eringen [18, 19] have been widely employed to predict the mechanical behavior of nanomaterials [20–26]. According to Eringen's nonlocal theory, the stress at the reference point x is a function of strain field at all points of the domain.

✉ Reza Ansari
r_ansari@guilan.ac.ir

✉ Jalal Torabi
jalal.torabii@gmail.com

[1] Department of Mechanical Engineering, University of Guilan, P.O. Box 3756, Rasht, Iran

Gibson et al. [27] indicated that the nonlocal elasticity theory can accurately predict the vibration behavior of nanostructures. Considering Eringen's nonlocal theory, various beam [25, 28–32] and shell [33–38] models have been used to study the mechanical behavior of carbon nanotubes. However, based on the nonlocal elasticity theory, a few studies have been done on the vibration and buckling of CNCs. Based on the nonlocal elasticity theory and using tapered rod model, Shu and Shau [39] studied the axial vibration of CNCs. Employing the modified Wentzel-Brillouin-Kramers (WBK) method, the axial vibration frequencies were obtained. Chang [40] investigated the small-scale effect on the axial vibration of nonuniform and nonhomogeneous nanorods based on the nonlocal continuum theory. Furthermore, Firouz-Abadi et al. [41, 42] presented the free vibration and stability analysis of CNCs using nonlocal shell model. Assuming the thin shell theories and employing the Galerkin technique, the effect of Eringen's nonlocal parameter on the natural frequency and buckling load of CNCs was examined. Based on the nonlocal continuum shell model, Fotouhi et al. [43] studied the free vibration of embedded CNCs. Considering Donnell's linear strain–displacement relations for thin shells and using Galerkin technique, the natural frequency of simply supported CNC was obtained. Moreover, Ansari et al. [44] analyzed the nonlocal vibration of CNCs using an analytical approach. Using the Galerkin method, the effects of boundary conditions, semi-vertex angle and nonlocal parameter on the natural frequency of CNCs were explored.

Recently, integral form of Eringen's nonlocal theory was used to investigate the bending of nanobeams [45, 46]. The paradoxical results were observed in the case of cantilever nanobeam where the integral formulation predicts the softening effect for nonlocal parameter, while the differential form results in stiffening effect. However, in the case of clamped or simply supported boundary conditions, integral and differential forms of nonlocal theory have the same trend and both of these formulations predict softening effect for nonlocal parameter.

In this paper, the vibration analysis of CNCs embedded in an elastic foundation is studied based on the differential formulation of nonlocal theory using the variational differential quadrature (VDQ) method. Since the VDQ method is directly applied to the variational form of governing equations, the derivation procedure of the differential form of equations is not needed. Based on the first-order shear deformation shell theory and considering the Eringen's nonlocal effect, the energy functional of the CNC is presented. Employing the generalized differential quadrature (GDQ) method in axial direction and periodic differential operators in circumferential direction, the energy functional is discretized. Eventually, using matrix relations and based on Hamilton's principle, the reduced forms of mass and stiffness matrices are easily obtained from the discretized form of energy functional. It should be noted that by applying the periodic differential operators in circumferential direction, the periodicity conditions are automatically satisfied. Utilizing this efficient numerical method, the effects of various boundary conditions on the vibrational behavior of CNCs can be easily examined. In addition, the influences of Winkler and Pasternak coefficients of elastic foundation, various semi-apex angles and nonlocal parameters on the natural frequency of CNCs are investigated.

2 Variational differential quadrature method

The description of variational differential quadrature method [47–49] is explained in this section. Hamilton's principle for a deformable body is presented by

$$\int_{t_1}^{t_2} \delta(W_{\mathrm{e}} + T - U)\mathrm{d}t = 0 \tag{1}$$

where δ is the first variation, W_e denotes the work of external loads, T is the kinetic energy and U presents the elastic strain energy. The external work and kinetic energy can be written as

$$W_{\mathrm{e}} = \int_A \mathbf{F}\cdot\mathbf{U}\mathrm{d}A = \int_A \mathbf{U}^{\mathrm{T}}\mathbf{F}\mathrm{d}A \tag{2}$$

$$T = \frac{1}{2}\int_\forall \rho\dot{\mathbf{U}}\cdot\dot{\mathbf{U}}\mathrm{d}\forall = \frac{1}{2}\int_\forall \dot{\mathbf{U}}^{\mathrm{T}}\rho\dot{\mathbf{U}}\mathrm{d}\forall \tag{3}$$

where $\mathbf{U}$ and $\mathbf{F}$ are arbitrary displacement and force vectors, respectively, ρ is the mass density and $(\dot{\cdot})$ defines the differentiation with respect to time. The elastic strain energy is written as

$$U = \frac{1}{2}\int_\forall \tilde{\sigma} : \tilde{\epsilon}\mathrm{d}\forall \tag{4}$$

in which $\tilde{\sigma}$ and $\tilde{\epsilon}$ are 3×3 symmetric stress and strain tensors, respectively. For a continuum elastic body, the Hooke's law is presented by

$$\tilde{\sigma}_{ij} = \tilde{C}_{ijkl}\tilde{\epsilon}_{kl} \tag{5}$$

where $\tilde{\mathbf{C}}$ is a symmetric fourth-order elasticity tensor. Using Voigt notation, Eq. (5) can be simplified to

$$\sigma = \mathbf{C}\epsilon \tag{6}$$

in which $\mathbf{C}$ is a material stiffness matrix, also $\boldsymbol{\sigma}$ and ϵ are as follows

$$\boldsymbol{\sigma} = [\tilde{\sigma}_{11} \quad \tilde{\sigma}_{22} \quad \tilde{\sigma}_{33} \quad \tilde{\sigma}_{23} \quad \tilde{\sigma}_{13} \quad \tilde{\sigma}_{12}]^{\mathrm{T}} \tag{7}$$

$$\epsilon = [\tilde{\varepsilon}_{11} \quad \tilde{\varepsilon}_{22} \quad \tilde{\varepsilon}_{33} \quad \gamma_{23} \quad \gamma_{13} \quad \gamma_{12}]^{\mathrm{T}} \tag{8}$$

Using Eqs. (6–8), the strain energy can be written as

$$U = \frac{1}{2}\int_{\forall} \epsilon \cdot \sigma d\forall = \frac{1}{2}\int_{\forall} \epsilon^{\mathrm{T}}\sigma d\forall = \frac{1}{2}\int_{\forall} \epsilon^{\mathrm{T}}\mathbf{C}\epsilon d\forall \tag{9}$$

The vector of strain given by Eq. (8) can be expressed as

$$\epsilon = \mathbf{EU} \tag{10}$$

where $\mathbf{E}$ is the matrix operator which includes the differential operators based on the strain–displacement relations.

In the VDQ method, the displacement components are discretized over space domain and the strain components are defined using numerical differential operators. The discretized strain vector is

$$\bar{\bar{\epsilon}} = \mathbb{E}\mathbb{U} \tag{11}$$

where $\bar{\bar{\epsilon}}$, $\mathbb{U}$ and $\mathbb{E}$ are the discretized forms of ϵ, $\mathbf{U}$ and $\mathbf{E}$, respectively. Introducing an accurate numerical row vector integral operator ($\tilde{\mathbb{S}}$) and following the mathematical approach described in [47], Eq. (9) can be written as

$$U = \frac{1}{2}\bar{\bar{\epsilon}}^{\mathrm{T}}(\mathbf{C}\otimes\mathbb{S})\bar{\bar{\epsilon}} \tag{12}$$

where $\mathbb{S} = \mathrm{diag}\left(\tilde{\mathbb{S}}\right)$. It is worth to note that when $\tilde{\mathbb{S}}$ is n components vector, $\mathrm{diag}\left(\tilde{\mathbb{S}}\right)$ returns the square matrix $\mathbb{S}$ of order n. Moreover, $\otimes$ introduces the Kronecker product [47]. By inserting Eq. (11) into (12), the strain energy is obtained as

$$U = \frac{1}{2}\mathbb{U}^{\mathrm{T}}\mathbb{E}^{\mathrm{T}}(\mathbf{C}\otimes\mathbb{S})\mathbb{E}\mathbb{U} \tag{13}$$

As well, the kinetic energy Eq. (3) and external work Eq. (2) can be written as

$$T = \frac{1}{2}\dot{\mathbb{U}}^{\mathrm{T}}\rho(\mathbf{I}\otimes\mathbb{S})\dot{\mathbb{U}} \tag{14}$$

$$W_{\mathrm{e}} = \mathbb{U}^{\mathrm{T}}(\mathbf{I}\otimes\mathbb{S})\tilde{\mathbb{F}} \tag{15}$$

in which $\mathbf{I}$ is the identity matrix and $\tilde{\mathbb{F}}$ stands for the discretized form of $\mathbf{F}$. Substituting Eqs. (13)–(15) into Hamilton's principle, one can obtain

$$\int_{t_1}^{t_2} \delta\left(\mathbb{U}^{\mathrm{T}}(\mathbf{I}\otimes\mathbb{S})\tilde{\mathbb{F}} + \frac{1}{2}\dot{\mathbb{U}}^{\mathrm{T}}\rho(\mathbf{I}\otimes\mathbb{S})\dot{\mathbb{U}} - \frac{1}{2}\mathbb{U}^{\mathrm{T}}\mathbb{E}^{\mathrm{T}}(\mathbf{C}\otimes\mathbb{S})\mathbb{E}\mathbb{U}\right)\mathrm{d}t = 0 \tag{16}$$

By taking the variation and considering the integration by parts in time domain, Eq. (16) becomes [47]

$$\int_{t_1}^{t_2} \left(\delta\mathbb{U}^{\mathrm{T}}(\mathbf{I}\otimes\mathbb{S})\tilde{\mathbb{F}} - \delta\mathbb{U}^{\mathrm{T}}\rho(\mathbf{I}\otimes\mathbb{S})\ddot{\mathbb{U}} - \delta\mathbb{U}^{\mathrm{T}}\mathbb{E}^{\mathrm{T}}(\mathbf{C}\otimes\mathbb{S})\mathbb{E}\mathbb{U}\right)\mathrm{d}t$$
$$= \int_{t_1}^{t_2} \delta\mathbb{U}^{\mathrm{T}}\left((\mathbf{I}\otimes\mathbb{S})\tilde{\mathbb{F}} - \rho(\mathbf{I}\otimes\mathbb{S})\ddot{\mathbb{U}} - \mathbb{E}^{\mathrm{T}}(\mathbf{C}\otimes\mathbb{S})\mathbb{E}\mathbb{U}\right)\mathrm{d}t = 0 \tag{17}$$

which results in

$$\rho(\mathbf{I}\otimes\mathbb{S})\ddot{\mathbb{U}} + \mathbb{E}^{\mathrm{T}}(\mathbf{C}\otimes\mathbb{S})\mathbb{E}\mathbb{U} - (\mathbf{I}\otimes\mathbb{S})\tilde{\mathbb{F}} = 0 \tag{18}$$

Equation (18) can be simplified to

$$\mathbb{M}\ddot{\mathbb{U}} + \mathbb{K}\mathbb{U} - \mathbb{F} = 0 \tag{19}$$

in which

$$\mathbb{M} = \rho(\mathbf{I}\otimes\mathbb{S}) \tag{20}$$

$$\mathbb{K} = \mathbb{E}^{\mathrm{T}}(\mathbf{C}\otimes\mathbb{S})\mathbb{E} \tag{21}$$

$$\mathbb{F} = (\mathbf{I}\otimes\mathbb{S})\tilde{\mathbb{F}} \tag{22}$$

3 Application of VDQ method in the nonlocal vibration of embedded nanocone

The vibration of CNCs resting on elastic foundation based on the nonlocal shell theory and employing the VDQ method is presented in this section. According to the nonlocal elasticity theory, the stress at a reference point x of a body is a function of the strain field at every point in the medium. On the basis of the nonlocal theory, the differential form of constitutive relation is given by

$$\left(1 - (e_0 a)^2\nabla^2\right)\sigma = \mathbf{C}\epsilon \tag{23}$$

The parameter $e_0 a$ denotes the nonlocal parameter which captures the size effects in small-scale structures.

The nanocone is modeled as a conical shell. Figure 1 shows the schematic of circular conical shell of small radius R_1, large radius R_2, thickness h, semi-apex angle β and length L. The displacement field based on the first-order shear deformation theory and considering in-plain movements is defined as

$$u = u_0(x,\theta,t) + z\psi_0(x,\theta,t),\; v = v_0(x,\theta,t) + z\phi_0(x,\theta,t),$$
$$w = w_0(x,\theta,t) \tag{24}$$

where u, v and w are the displacement components along the x, θ and z direction, u_0, v_0 and w_0 denote the displacement of a point on the natural axis, ψ_0 and ϕ_0 stand for the rotations about θ and x directions, respectively. Equation (24) can be written as

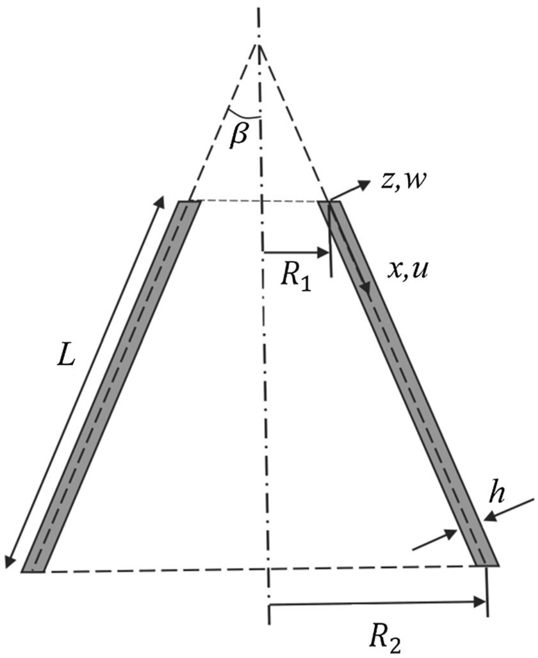

Fig. 1 Geometry and coordinate system of nanocone

$$\tilde{\mathbf{U}}=\begin{bmatrix} u \\ v \\ w \end{bmatrix}=\tilde{\mathbf{A}}\mathbf{U},\ \ \tilde{\mathbf{A}}=\begin{bmatrix} 1 & 0 & 0 & z & 0 \\ 0 & 1 & 0 & 0 & z \\ 0 & 0 & 1 & 0 & 0 \end{bmatrix},\quad \mathbf{U}=\begin{bmatrix} u_0 \\ v_0 \\ w_0 \\ \psi_0 \\ \phi_0 \end{bmatrix} \tag{25}$$

in which $\tilde{\mathbf{U}}$ is the displacement vector and $\mathbf{U}$ is the augmented displacement vector. According to displacement field, the strain components of nanocone can be written as

$$\begin{aligned}
\tilde{\epsilon}_{11} &= \frac{\partial u_0}{\partial x}+z\frac{\partial \psi_0}{\partial x},\\
\tilde{\epsilon}_{22} &= \frac{1}{R(x)}\frac{\partial v_0}{\partial \theta}+\frac{u_0 \sin(\beta)}{R(x)}+\frac{w_0\cos(\beta)}{R(x)}\\
&\quad +z\left(\frac{\psi_0 \sin(\beta)}{R(x)}+\frac{1}{R(x)}\frac{\partial \phi_0}{\partial \theta}\right),\\
\tilde{\epsilon}_{33} &= 0,\\
\gamma_{12} = 2\tilde{\epsilon}_{12} &= \frac{1}{R(x)}\frac{\partial u_0}{\partial \theta}+\frac{\partial v_0}{\partial x}-\frac{v_0 \sin(\beta)}{R(x)}\\
&\quad +z\left(\frac{1}{R(x)}\frac{\partial \psi_0}{\partial \theta}+\frac{\partial \phi_0}{\partial x}-\frac{\phi_0 \sin(\beta)}{R(x)}\right),\\
\gamma_{12} = 2\tilde{\epsilon}_{12} &= \frac{1}{R(x)}\frac{\partial u_0}{\partial \theta}+\frac{\partial v_0}{\partial x}-\frac{v_0 \sin(\beta)}{R(x)}\\
&\quad +z\left(\frac{1}{R(x)}\frac{\partial \psi_0}{\partial \theta}+\frac{\partial \phi_0}{\partial x}-\frac{\phi_0 \sin(\beta)}{R(x)}\right),\\
\gamma_{23} = 2\tilde{\epsilon}_{23} &= \frac{1}{R(x)}\frac{\partial w_0}{\partial \theta}-\frac{v_0 \cos(\beta)}{R(x)}\\
&\quad +\phi_0, \gamma_{13} = 2\tilde{\epsilon}_{13} = \frac{\partial w_0}{\partial x}+\psi_0
\end{aligned} \tag{26}$$

where $R(x)=R_1+x\sin(\beta)$. Considering nonzero components from above equations, the strain vector can be defined as

$$\epsilon = (\mathbf{E}+\mathbf{BH})\mathbf{U} \tag{27}$$

where

$$\mathbf{E}=\begin{bmatrix} \frac{\partial}{\partial x} & 0 & 0 & 0 & 0 \\ \frac{\sin(\beta)}{R(x)} & \frac{1}{R(x)}\frac{\partial}{\partial \theta} & \frac{\cos(\beta)}{R(x)} & 0 & 0 \\ \frac{1}{R(x)}\frac{\partial}{\partial \theta} & \frac{\partial}{\partial x}-\frac{\sin(\beta)}{R(x)} & 0 & 0 & 0 \\ 0 & -\frac{\cos(\beta)}{R(x)} & \frac{1}{R(x)}\frac{\partial}{\partial \theta} & 0 & 1 \\ 0 & 0 & \frac{\partial}{\partial x} & 1 & 0 \end{bmatrix}, \tag{28}$$

$$\mathbf{H}=\begin{bmatrix} 0 & 0 & 0 & \frac{\partial}{\partial x} & 0 \\ 0 & 0 & 0 & \frac{\sin(\beta)}{R(x)} & \frac{1}{R(x)}\frac{\partial}{\partial \theta} \\ 0 & 0 & 0 & \frac{1}{R(x)}\frac{\partial}{\partial \theta} & \frac{\partial}{\partial x}-\frac{\sin(\beta)}{R(x)} \\ 0 & 0 & 0 & 0 & 0 \\ 0 & 0 & 0 & 0 & 0 \end{bmatrix}, \tag{29}$$

$$\mathbf{B}=\mathrm{diag}([z \quad z \quad z \quad 0 \quad 0]) \tag{30}$$

in which ϵ denotes the strain vector and $\mathbf{E}$ and $\mathbf{H}$ are introduced as the strain matrix operators.

Using Eq. (9), the elastic strain energy is obtained as

$$\begin{aligned}
U &= \frac{1}{2}\int_{\forall} \mathbf{U}^{\mathrm{T}}(\mathbf{E}^{\mathrm{T}}\mathbf{CE}+\mathbf{E}^{\mathrm{T}}\mathbf{CBH}+\mathbf{H}^{\mathrm{T}}\mathbf{BCE}+\mathbf{H}^{\mathrm{T}}\mathbf{BCBH})\mathbf{U}\mathrm{d}\forall\\
&= \frac{1}{2}\int_{A} \mathbf{U}^{\mathrm{T}}\left(\mathbf{E}^{\mathrm{T}}\left(\int \mathbf{C}\mathrm{d}z\right)\mathbf{E}+\mathbf{E}^{\mathrm{T}}\left(\int \mathbf{CB}\mathrm{d}z\right)\mathbf{H}+\mathbf{H}^{\mathrm{T}}\left(\int \mathbf{BC}\mathrm{d}z\right)\mathbf{E}\right.\\
&\quad \left.+\mathbf{H}^{\mathrm{T}}\left(\int \mathbf{BCB}\mathrm{d}z\right)\mathbf{H}\right)\mathbf{U}\mathrm{d}A\\
&= \frac{1}{2}\int_{A} \mathbf{U}^{\mathrm{T}}(\mathbf{E}^{\mathrm{T}}\bar{\mathbf{C}}_1\mathbf{E}+\mathbf{E}^{\mathrm{T}}\bar{\mathbf{C}}_2\mathbf{H}+\mathbf{H}^{\mathrm{T}}\bar{\mathbf{C}}_2\mathbf{E}+\mathbf{H}^{\mathrm{T}}\bar{\mathbf{C}}_3\mathbf{H})\mathbf{U}\mathrm{d}A
\end{aligned} \tag{31}$$

where A is the cross-sectional area, $\mathrm{d}A=(R_1+x\sin(\beta))\mathrm{d}x\mathrm{d}\theta$. Considering homogeneous material for nanocone, one can write the stiffness matrix as

$$\mathbf{C}=\frac{E}{(1+v)}\begin{bmatrix} \frac{1}{1-v} & \frac{v}{1-v} & 0 & 0 & 0 \\ \frac{v}{1-v} & \frac{1}{1-v} & 0 & 0 & 0 \\ 0 & 0 & 1/2 & 0 & 0 \\ 0 & 0 & 0 & k_s/2 & 0 \\ 0 & 0 & 0 & 0 & k_s/2 \end{bmatrix} \tag{32}$$

where E is Young's modulus, v is Poisson's ratio and k_s stands for the shear correction factor. The constants $\bar{\mathbf{C}}_1$, $\bar{\mathbf{C}}_2$ and $\bar{\mathbf{C}}_3$ become

$$\bar{\mathbf{C}}_1 = \int \mathbf{C} dz, \quad \bar{\mathbf{C}}_2 = \int \mathbf{CB} dz, \quad \bar{\mathbf{C}}_3 = \int \mathbf{BCB} dz \tag{33}$$

It should be noted that considering the homogeneous material, the coefficient $\bar{\mathbf{C}}_2$ vanishes. Based on Eq. (3) and considering the nonlocal effects, the kinetic energy is calculated as

$$T = \frac{1}{2}\int_A \left(\dot{\mathbf{U}}^{\mathrm{T}}\rho\dot{\mathbf{U}} + (e_0\alpha)^2\dot{\mathbf{U}}^{\mathrm{T}}(\mathbf{G}_1^{\mathrm{T}}\rho\mathbf{G}_1 + \mathbf{G}_2^{\mathrm{T}}\rho\mathbf{G}_2\right)\mathrm{d}A \tag{34}$$

where $\mathbf{G}_1$, $\mathbf{G}_2$ and the inertia matrix ρ are obtained as

$$\mathbf{G}_1 = \begin{bmatrix} \frac{\partial}{\partial x} & 0 & 0 & 0 & 0 \\ 0 & \frac{\partial}{\partial x} & 0 & 0 & 0 \\ 0 & 0 & \frac{\partial}{\partial x} & 0 & 0 \\ 0 & 0 & 0 & \frac{\partial}{\partial x} & 0 \\ 0 & 0 & 0 & 0 & \frac{\partial}{\partial x} \end{bmatrix},$$

$$\mathbf{G}_2 = \begin{bmatrix} \frac{1}{R(x)}\frac{\partial}{\partial\theta} & 0 & 0 & 0 & 0 \\ 0 & \frac{1}{R(x)}\frac{\partial}{\partial\theta} & 0 & 0 & 0 \\ 0 & 0 & \frac{1}{R(x)}\frac{\partial}{\partial\theta} & 0 & 0 \\ 0 & 0 & 0 & \frac{1}{R(x)}\frac{\partial}{\partial\theta} & 0 \\ 0 & 0 & 0 & 0 & \frac{1}{R(x)}\frac{\partial}{\partial\theta} \end{bmatrix} \tag{35}$$

$$\boldsymbol{\rho} = \int_{\mathbf{A}} \tilde{\mathbf{A}}^{\mathbf{T}}\rho\tilde{\mathbf{A}}\mathbf{dz} \tag{36}$$

By studying the free vibration of nanocones, the external work vanishes. In addition, considering the nonlocal effects, the strain energy due to the Winkler and Pasternak coefficients of elastic foundation can be defined as:

$$U_F = \frac{1}{2}\int_\forall \mathbf{U}^{\mathrm{T}}(\mathbf{L}^{\mathrm{T}}\mathbf{Q}_1\mathbf{L} + (\mathrm{e}_0\alpha)^2\mathbf{P}^{\mathrm{T}}\mathbf{Q}_2\mathbf{P})\mathbf{U}\mathrm{d}A \tag{37}$$

in which

$$\mathbf{L} = \begin{bmatrix} 0 & 0 & 1 & 0 & 0 \\ 0 & 0 & \frac{\partial}{\partial x} & 0 & 0 \\ 0 & 0 & \frac{1}{R(x)}\frac{\partial}{\partial\theta} & 0 & 0 \end{bmatrix}, \tag{38}$$

$$\mathbf{P} = \begin{bmatrix} 0 & 0 & \frac{\partial}{\partial x} & 0 & 0 \\ 0 & 0 & \frac{1}{R(x)}\frac{\partial}{\partial\theta} & 0 & 0 \\ 0 & 0 & \frac{\partial^2}{\partial x^2} & 0 & 0 \\ 0 & 0 & \frac{\sin(\beta)}{R(x)}\frac{\partial}{\partial x} & 0 & 0 \\ 0 & 0 & \frac{1}{R(x)^2}\frac{\partial^2}{\partial\theta^2} & 0 & 0 \end{bmatrix}, \tag{39}$$

$$\mathbf{Q}_1 = \begin{bmatrix} k_w & 0 & 0 \\ 0 & k_g & 0 \\ 0 & 0 & k_g \end{bmatrix}, \mathbf{Q}_2 = \begin{bmatrix} k_w & 0 & 0 & 0 & 0 \\ 0 & k_w & 0 & 0 & 0 \\ 0 & 0 & k_g & 0 & 0 \\ 0 & 0 & 0 & k_g & 0 \\ 0 & 0 & 0 & 0 & k_g \end{bmatrix} \tag{40}$$

where k_w and k_g are Winkler and Pasternak coefficients of elastic foundation, respectively. Eventually, by inserting Eqs. (31), (34) and (37) into Hamilton's principle, one can write

$$\begin{aligned} &\int_{t_1}^{t_2} \delta \int_A \Big(\frac{1}{2}\dot{\mathbf{U}}^{\mathrm{T}}\rho\dot{\mathbf{U}} + \frac{1}{2}(e_0\alpha)^2\dot{\mathbf{U}}^{\mathrm{T}}\left[\mathbf{G}_1^{\mathrm{T}}\rho\mathbf{G}_1 + \mathbf{G}_2^{\mathrm{T}}\rho\mathbf{G}_2\right]\dot{\mathbf{U}} \\ &+\frac{1}{2}\mathbf{U}^{\mathrm{T}}\left(\mathbf{E}^{\mathrm{T}}\bar{\mathbf{C}}_1\mathbf{E} + \mathbf{H}^{\mathrm{T}}\bar{\mathbf{C}}_3\mathbf{H}\right)\mathbf{U} \\ &+\frac{1}{2}\mathbf{U}^{\mathrm{T}}(\mathbf{L}^{\mathrm{T}}\mathbf{Q}_1\mathbf{L} + (e_0\alpha)^2\mathbf{P}^{\mathrm{T}}\mathbf{Q}_2\mathbf{P})\mathbf{U}\Big)\mathrm{d}A\mathrm{d}t \end{aligned} \tag{41}$$

Employing the VDQ method, the discretized form of Eq. (41) can be written as

$$\begin{aligned} &\int_{t_1}^{t_2} \delta(\dot{\mathbb{U}}^{\mathrm{T}}(\boldsymbol{\rho}\otimes\mathbb{S})\dot{\mathbb{U}} + \frac{1}{2}(e_0\alpha)^2\dot{\mathbb{U}}^{\mathrm{T}} \\ &\times\left[\mathbb{G}_1^{\mathrm{T}}(\boldsymbol{\rho}\otimes\mathbb{S})\mathbb{G}_1 + \mathbb{G}_2^{\mathrm{T}}(\boldsymbol{\rho}\otimes\mathbb{S})\mathbb{G}_2\right]\dot{\mathbb{U}} \\ &+\frac{1}{2}\mathbb{U}^{\mathrm{T}}\left(\mathbb{E}^{\mathrm{T}}\left(\bar{\mathbf{C}}_1\otimes\mathbb{S}\right)\mathbb{E} + \mathbb{H}^{\mathrm{T}}\left(\bar{\mathbf{C}}_3\otimes\mathbb{S}\right)\mathbb{H}\right)\mathbb{U} \\ &+\frac{1}{2}\mathbb{U}^{\mathrm{T}}(\mathbb{L}^{\mathrm{T}}(\mathbf{Q}_1\otimes\mathbb{S})\mathbb{L} \\ &+(\mathrm{e}_0\alpha)^2\mathbb{P}^{\mathrm{T}}(\mathbf{Q}_2\otimes\mathbb{S})\mathbb{P})\mathbb{U}\Big)dt \end{aligned} \tag{42}$$

Taking the variation and considering the integration by parts in time domain results in [47]

$$\mathbb{M}\ddot{\mathbb{U}} + \mathbb{K}\mathbb{U} = 0 \tag{43}$$

where the mass matrix $\mathbb{M}$ and stiffness matrix $\mathbb{K}$ are defined as follows

$$\begin{aligned} \mathbb{M} &= \boldsymbol{\rho}\otimes\mathbb{S} + (e_0\alpha)^2\left[\mathbb{G}_1^{\mathrm{T}}(\boldsymbol{\rho}\otimes\mathbb{S})\mathbb{G}_1 + \mathbb{G}_2^{\mathrm{T}}(\boldsymbol{\rho}\otimes\mathbb{S})\mathbb{G}_2\right], \\ \mathbb{K} &= \mathbb{E}^{\mathrm{T}}\left(\bar{\mathbf{C}}_1\otimes\mathbb{S}\right)\mathbb{E} + \mathbb{H}^{\mathrm{T}}\left(\bar{\mathbf{C}}_3\otimes\mathbb{S}\right)\mathbb{H} \\ &\quad + \mathbb{L}^{\mathrm{T}}(\mathbf{Q}_1\otimes\mathbb{S})\mathbb{L} + (e_0\alpha)^2\mathbb{P}^{\mathrm{T}}(\mathbf{Q}_2\otimes\mathbb{S})\mathbb{P} \end{aligned} \tag{44}$$

in which the two-dimensional integral operator $\mathbb{S}$ is written as

$$\mathbb{S} = \mathbf{S}_\theta \otimes (\mathbf{S}_x \mathbf{R}) \tag{45}$$

where $\mathbf{S}_\theta$ and $\mathbf{S}_x$ are the integral operators in circumferential and axial direction, respectively. In addition, the discretized matrix operators $\mathbb{G}_1$, $\mathbb{G}_2$, $\mathbb{E}$, $\mathbb{H}$, $\mathbb{L}$ and $\mathbb{P}$ are as follows

$$\mathbb{G}_1 = \mathbf{I}_{5\times5} \otimes \mathbf{D}_x^{(1)}, \quad \mathbb{G}_2 = \mathbf{I}_{5\times5} \otimes \left(\mathbf{R}\mathbf{D}_\theta^{(1)}\right) \tag{46}$$

$$\mathbb{E} = \begin{bmatrix} \bar{\mathbf{D}}_x^{(1)} & 0 & 0 & 0 & 0 \\ \sin(\beta)\mathbf{R}\mathbf{D}^0 & \mathbf{R}\mathbf{D}_\theta^{(1)} & \cos(\beta)\mathbf{R}\mathbf{D}^0 & 0 & 0 \\ \mathbf{R}\mathbf{D}_\theta^{(1)} & \bar{\mathbf{D}}_x^{(1)} - \sin(\beta)\mathbf{R}\mathbf{D}^0 & 0 & 0 & 0 \\ 0 & -\cos(\beta)\mathbf{R}\mathbf{D}^0 & \mathbf{R}\mathbf{D}_\theta^{(1)} & 0 & \bar{\mathbf{D}}^0 \\ 0 & 0 & \bar{\mathbf{D}}_x^{(1)} & \bar{\mathbf{D}}^0 & 0 \end{bmatrix} \tag{47}$$

$$\mathbb{H} = \begin{bmatrix} 0 & 0 & 0 & \bar{\mathbf{D}}_x^{(1)} & 0 \\ 0 & 0 & 0 & \sin(\beta)\mathbf{R}\mathbf{D}^0 & \mathbf{R}\mathbf{D}_\theta^{(1)} \\ 0 & 0 & 0 & \mathbf{R}\mathbf{D}_\theta^{(1)} & \bar{\mathbf{D}}_x^{(1)} - \sin(\beta)\mathbf{R}\mathbf{D}^0 \\ 0 & 0 & 0 & 0 & 0 \\ 0 & 0 & 0 & 0 & 0 \end{bmatrix} \tag{48}$$

$$\mathbb{L} = \begin{bmatrix} 0 & 0 & \bar{\mathbf{D}}^0 & 0 & 0 \\ 0 & 0 & \bar{\mathbf{D}}_x^{(1)} & 0 & 0 \\ 0 & 0 & \mathbf{R}\mathbf{D}_\theta^{(1)} & 0 & 0 \end{bmatrix} \tag{49}$$

$$\mathbb{P} = \begin{bmatrix} 0 & 0 & \bar{\mathbf{D}}_x^{(1)} & 0 & 0 \\ 0 & 0 & \mathbf{R}\mathbf{D}_\theta^{(1)} & 0 & 0 \\ 0 & 0 & \bar{\mathbf{D}}_x^{(2)} & 0 & 0 \\ 0 & 0 & \sin(\beta)\mathbf{R}\mathbf{D}_x^{(1)} & 0 & 0 \\ 0 & 0 & \bar{\bar{\mathbf{R}}}\bar{\mathbf{D}}_\theta^{(2)} & 0 & 0 \end{bmatrix} \tag{50}$$

where

$$\begin{aligned} \bar{\mathbf{D}}_x^{(n)} &= \mathbf{I}_\theta \otimes \mathbf{D}_x^{(n)}, \quad n = 1,2 \\ \bar{\mathbf{D}}_\theta^{(n)} &= \mathbf{D}_\theta^{(n)} \otimes \mathbf{I}_x, \quad n = 1,2 \\ \bar{\mathbf{D}}^0 &= \mathbf{I}_\theta \otimes \mathbf{I}_x \end{aligned} \tag{51}$$

and

$$\begin{aligned} \mathbf{R} &= R_1 + \mathrm{diag}(\sin(\beta)[x_1 x_2 \ldots x_{n_1}]) \\ \bar{\mathbf{R}} &= \mathrm{diag}\left(\mathrm{diag}(\mathbf{I}_\theta) \otimes \left(\begin{bmatrix} \frac{1}{R_1 + x_1\sin(\beta)} \\ \frac{1}{R_1 + x_2\sin(\beta)} \\ \vdots \\ \frac{1}{R_1 + x_{n_1}\sin(\beta)} \end{bmatrix}\right)\right) \\ \bar{\bar{\mathbf{R}}} &= \mathrm{diag}\left(\mathrm{diag}(\mathbf{I}_\theta) \otimes \left(\begin{bmatrix} \frac{1}{(R_1 + x_1\sin(\beta))^2} \\ \frac{1}{(R_1 + x_2\sin(\beta))^2} \\ \vdots \\ \frac{1}{(R_1 + x_{n_1}\sin(\beta))^2} \end{bmatrix}\right)\right) \end{aligned} \tag{52}$$

where $\mathbf{I}_x$ and $\mathbf{I}_\theta$ are identity matrices with the size $n_1 \times n_1$ and $n_2 \times n_2$ in which n_1 and n_2 are the numbers of grid points in x and θ directions, respectively. Furthermore, $\mathbf{D}_x^{(n)}$ and $\mathbf{D}_\theta^{(n)}$ are the differential operators in axial and circumferential directions, respectively. The superscript n denotes the order of differentiation. In this study, the differential and integral operators in x direction are defined based on the GDQ method, while the periodic differential operators are used in θ direction. In this regard, the GDQ method and periodic differential operators are presented in the next section.

4 Differential and integral operators

4.1 GDQ method

On the basis of the GDQ method [50], the nth derivative of function $f(x)$ is specified as a linear sum of the function, i.e.,

$$\left.\frac{\partial^n f(x)}{\partial x^n}\right|_{x=x_i} = \sum_{j=1}^{n_1} \varsigma_{ij}^n f(x_j), \; i = 1,2,\ldots,n_1 \tag{53}$$

in which ς_{ij}^n is the weighting coefficients. A column vector $\mathbf{F}$ can be given as

$$\mathbf{F} = [F_j] = [f(x_j)] = [f(x), f(x_2), \ldots, f(x_{n_1})]^T \tag{54}$$

where $f(x_j)$ is the nodal values of $f(x)$ at $x = x_j$. According to Eq. (53), a differential matrix operator can be written as

$$\frac{\partial^n}{\partial x^n}(\mathbf{F}) = \mathbf{D}_x^{(n)}\mathbf{F} = \left[D_x^{(n)}\right]_{i,j}\{F_j\} \tag{55}$$

where

$$\mathbf{D}_x^{(n)} = \left[D_x^{(n)}\right]_{i,j} = \varsigma_{ij}^n, i,j = 1 : n_1 \tag{56}$$

In Eq. (56), ς_{ij}^n is calculated by [50]

$$\varsigma_{ij}^n = \begin{cases} I_{ij}, & n = 0 \\ \dfrac{\mathcal{L}(x_i)}{(x_i - x_j)\mathcal{L}(x_j)}, & \begin{cases} i \neq j \text{ and } i,j = 1,\ldots,n_1 \\ n = 1 \end{cases} \\ n\left[\varsigma_{ij}^1 \varsigma_{ii}^{n-1} - \dfrac{\varsigma_{ij}^{n-1}}{x_i - x_j}\right], & \begin{cases} i \neq j \text{ and } i,j = 1,\ldots,n_1 \\ n = 2,3,\ldots,n_1 - 1 \end{cases} \\ -\displaystyle\sum_{j=1;j\neq i}^{n_1} \varsigma_{ij}^n, & \begin{cases} i = j \text{ and } i,j = 1,\ldots,n_1 \\ n = 1,2,\ldots,n_1 - 1 \end{cases} \end{cases} \tag{57}$$

in which I_{ij} is the components of a $n_1 \times n_1$ identity matrix and $\mathcal{L}(x_i)$ is given as

$$\mathcal{L}(x_i) = \prod_{j=1;j\neq i}^{n_1} (x_i - x_j) \tag{58}$$

Previous studies [51] indicated that the Chebyshev-Gauss–Lobatto grid point distribution has the most convergence and stability. Consequently, the grid points in axial direction can be generated as

$$x_i = \frac{1}{2}\left(1 - \cos\frac{i-1}{n_1 - 1}\pi\right)L \tag{59}$$

Utilizing the Taylor series and the GDQ method, an accurate integral operator can be defined as [47]

$$\mathbf{S}_x = \sum_{n=1}^{n_1-1} \mathbf{X}^{(n)}\mathbf{D}_x^{(n)} \tag{60}$$

where the row vector $\mathbf{X}^{(n)}$ is given as

$$\mathbf{X}^{(n)} = \left[\frac{(x_2 - x_1)^{n+1}}{2^{n+1}(n+1)!}\cdots\frac{(x_{i+1} - x_i)^{n+1} - (x_{i-1} - x_i)^{n+1}}{2^{n+1}(n+1)!}\cdots\frac{(x_{n_1-1} - x_{n_1})^{n+1}}{2^{n+1}(n+1)!}\right] \tag{61}$$

4.2 Periodic operators

The displacement components are periodic in circumferential direction; therefore, using the periodic differential operators in this direction naturally satisfies the periodicity condition. Assuming a periodic grid points between 0 and 2π and employing the derivatives of periodic sinc function as a base function in a collocation method, the differential matrix operators are attained. The periodic differential matrix operators ($\mathbf{D}_\theta^{(n)}$) are defined as [52]

$$\mathbf{D}_\theta^{(1)} = \left[a_{i,j}\right], \quad \mathbf{D}_\theta^{(2)} = \left[b_{i,j}\right], \tag{62}$$

where the coefficients $a_{i,j}$ and $b_{i,j}$ are given as

$$\begin{cases} a_{11} = 0 \\ a_{i,1} = \dfrac{(-1)^{i-1}}{2}\cot\dfrac{\pi(i-1)}{n_2} \\ a_{1,j} = \dfrac{(-1)^{n_2-j+1}}{2}\cot\dfrac{\pi(n_2-j+1)}{n_2} \\ a_{i+1,j+1} = a_{i,j} \end{cases}, \quad i,j = 2,\ldots,n_2 \tag{63}$$

$$\begin{cases} b_{11} = -\dfrac{n_2^2}{12} - \dfrac{1}{6} \\ b_{i,1} = \dfrac{(-1)^{i-2}}{2\sin^2\dfrac{\pi(i-1)}{n_2}} \\ b_{1,j} = \dfrac{(-1)^{n_2-j}}{2\sin^2\dfrac{\pi(n_2-j+1)}{n_2}} \\ b_{i+1,j+1} = b_{i,j} \end{cases}, \quad j = 2,\ldots,n_2 \tag{64}$$

In addition, considering the periodic grid points in circumferential direction, the integral operator in this direction is defined as

$$\mathbf{S}_\theta = \left[\frac{2\pi}{n_2}\cdots\frac{2\pi}{n_2}\right]_{1\times n_2} \tag{65}$$

5 Results and Discussion

The vibrational analysis of carbon nanocones resting on elastic foundation based on Eringen's nonlocal elasticity theory is presented. Various studies revealed that the mechanical properties of CNCs such as Young's modulus and Poisson's ratio depend on the apex angle of cone and can be obtained as follows [10, 44, 53, 54]: $E = 0.89\cos^4(\beta)$ TPa and $\nu = 0.25\sin^2(\beta)$. Moreover, the mass density is $\rho = 2237\ \mathrm{Kg/m^3}$ [10, 44] and the wall thickness is considered to be $h = 0.34$ nm. As both Winkler and Pasternak coefficients of elastic medium are taken into account, the nondimensional coefficients are given as

$$\begin{aligned} K_w &= \frac{k_w R_2^4}{D} \\ K_g &= \frac{k_g R_2^2}{D} \end{aligned} \tag{66}$$

where $D = \frac{Eh^3}{12(1-\nu^2)}$ is the bending rigidity. Since the carbon nanocone is modeled as a conical shell, the accuracy of the present study is verified by comparing the natural frequencies of the conical shell with the values predicted by Tornabene [51]. In this regard, the first ten frequency parameters ($\Omega = \omega R_2\sqrt{\rho(1-\nu^2)/E}$) for different boundary conditions are compared in Table 1. As it can be seen, the results have good agreement. In addition, the natural frequencies of simply supported (SS) CNCs are compared with the results obtained by the molecular mechanics (MM) approach [13] for various nonlocal parameters and apex angles in Fig. 2. It can be seen that the fundamental frequencies of CNCs with different apex angles need various nonlocal parameters to be matched with the values obtained by MM approach. In addition, neglecting the nonlocal effect generally leads to over-predict the natural frequencies.

Figure 3 shows the fundamental frequencies of CNC versus length-to-small radius ratio for various nonlocal parameters and boundary conditions. It reveals that the fundamental frequency of CNCs decreases when the length-to-radius ratio increases. Moreover, considering the nonlocal effects decreases the natural frequencies and this effect is more significant for smaller L/R_1 ratios, while for nanocones with the larger length, one can neglect the

Table 1 Comparison of dimensionless frequency parameter ($\Omega = \omega R_2\sqrt{\rho(1-\nu^2)/E}$) of conical shell for different boundary conditions ($R_1 = 0.5$ m, $h = 0.1$ m, $\beta = 40$, $L\cos(\beta) = 2$ m)

Mode no.	CC		SS		CS	
	Present study	Ref. [51]	Present study	Ref. [51]	Present study	Ref. [51]
1	0.573	0.573	0.525	0.525	0.567	0.568
2	0.573	0.573	0.525	0.525	0.567	0.568
3	0.603	0.603	0.560	0.560	0.591	0.591
4	0.603	0.603	0.560	0.560	0.591	0.591
5	0.693	0.693	0.630	0.630	0.692	0.692
6	0.693	0.693	0.630	0.630	0.692	0.692
7	0.840	0.840	0.800	0.800	0.835	0.835
8	0.840	0.840	0.800	0.800	0.835	0.835
9	0.882	0.882	0.802	0.802	0.882	0.882
10	0.882	0.882	0.802	0.802	0.882	0.882

nonlocal effect. Also, boundary conditions play an important role on the size-dependent behavior of CNCs, as by assuming the clamped-free (CF) boundary condition, one can neglect the nonlocal effect for $L/R_1 \geq 6$, while this ratio is larger than 6 for simply supported (SS), clamped-simply supported (CS) and clamped–clamped (CC) boundary conditions.

The effects of elastic foundation coefficients on the vibrational behavior of simply supported CNC are demonstrated in Figs. 4–6 for different nonlocal parameters, length-to-radius ratios and apex angles, respectively. Winkler and Pasternak coefficients effects are examined separately. As it is observed, the presence of the elastic foundation increases the natural frequencies of CNC. Figure 4 indicates that the increase in elastic foundation coefficients reduces the size-dependency of the natural frequencies of CNC. Results of Figs. 5 and 6 imply that the influences of elastic foundations on the fundamental frequency are more significant for smaller length-to-radius ratios and apex angles. Furthermore, for the larger values of L/R_1 ratios and apex angles, the increase in natural frequencies with the rise of elastic foundation coefficients is not considerable.

Natural frequencies of CNCs versus mode numbers for various nonlocal parameters and boundary conditions are depicted in Fig. 7. It is apparent that clamped–clamped boundary condition gives the highest natural frequency. In addition, the effects of nonlocal parameters are more considerable in the higher mode numbers.

The influences of various nonlocal parameters, boundary conditions and elastic foundation coefficients on the fundamental frequency (THz) of embedded CNC are accounted in Table 2. The results reveal that by considering the fully simply supported boundary condition, the natural frequencies are more influenced by the alternations of the elastic foundation coefficients. On the other hand, neglecting the elastic medium, the fundamental frequency of clamped-free CNC is less size dependent.

6 Conclusion

Based on the nonlocal elasticity theory, the vibrational behavior of CNCs embedded in an elastic foundation was studied. Considering the first-order shear deformation theory, employing Hamilton's principle and using the VDQ method, the discretized form of governing equations was derived. Discretization procedure of the energy functional was presented using the GDQ method in axial direction and periodic differential operators in circumferential direction. Young's modulus and Poisson's ratio of CNCs were considered to vary with the apex angle, according to previous studies. The results of this study were validated with those given in the literature. Furthermore, employing an efficient numerical method, the effects of various boundary conditions, semi-apex angles, nonlocal parameters and both Winkler and Pasternak coefficients of elastic foundation were examined on the natural frequencies of CNCs.

As observed, the nonlocal parameter has important effects on the vibrational behavior of embedded CNCs. Comparing the results with those given by molecular mechanics approach revealed that classical continuum mechanics generally over-predict the natural frequencies of CNCs. Furthermore, geometrical parameters such as length and apex angle of nanocones play an important role on the size-dependent natural frequencies, as the increase in length-to-radius ratio and apex angle of nanocone makes the structure more flexible and reduces the fundamental frequencies. Also, by increasing the L/R_1 ratio, one can neglect the nonlocal effects.

Moreover, the influences of elastic medium coefficients on the fundamental frequencies of CNCs were accounted

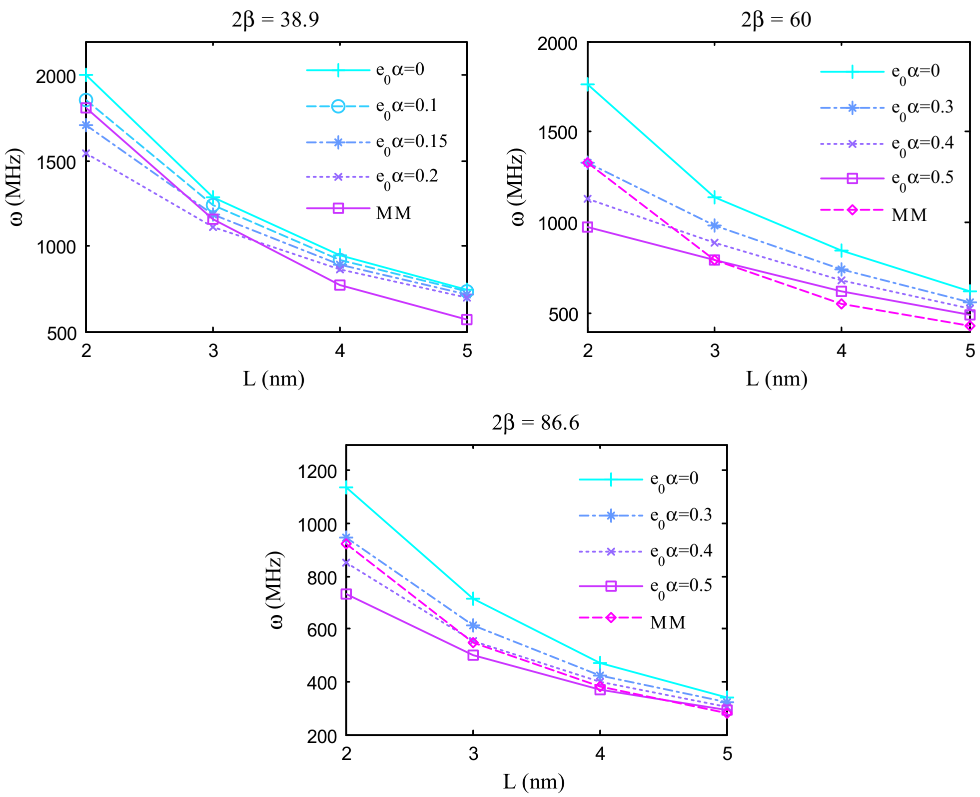

Fig. 2 Comparison of natural frequencies of simply supported CNC with the results obtained by molecular mechanics (MM) $\left(\frac{R_1}{h} = 0.1\right)$

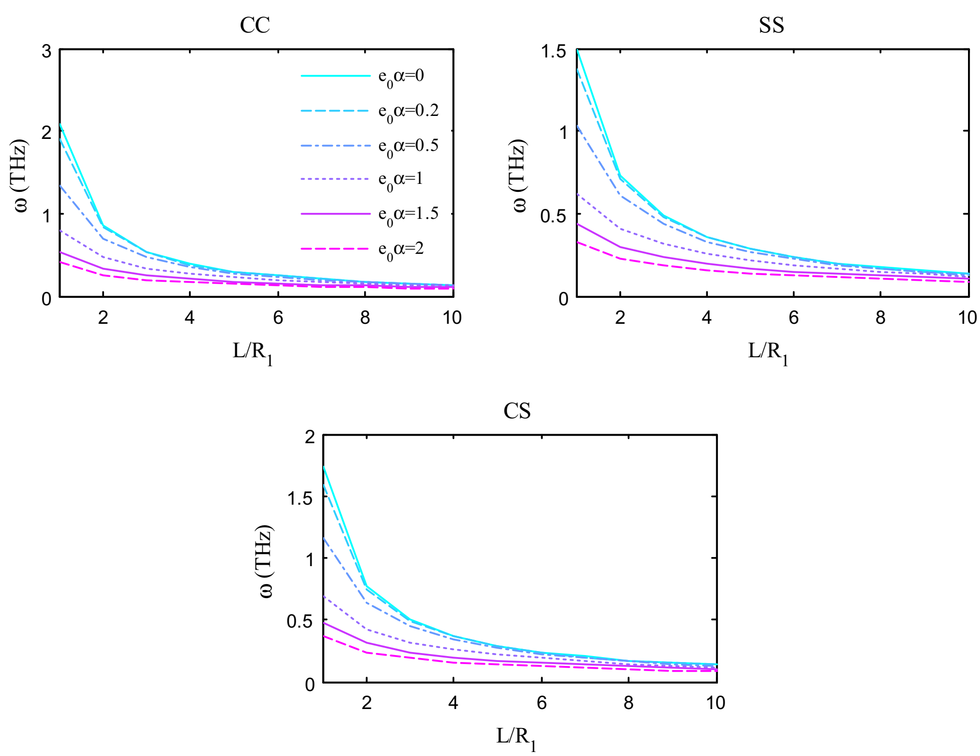

Fig. 3 Fundamental frequencies of CNC versus length-to-small radius ratio $\left(\frac{R_1}{h} = 5, 2\beta = 38.9,\ K_w = 0, K_g = 0\right)$

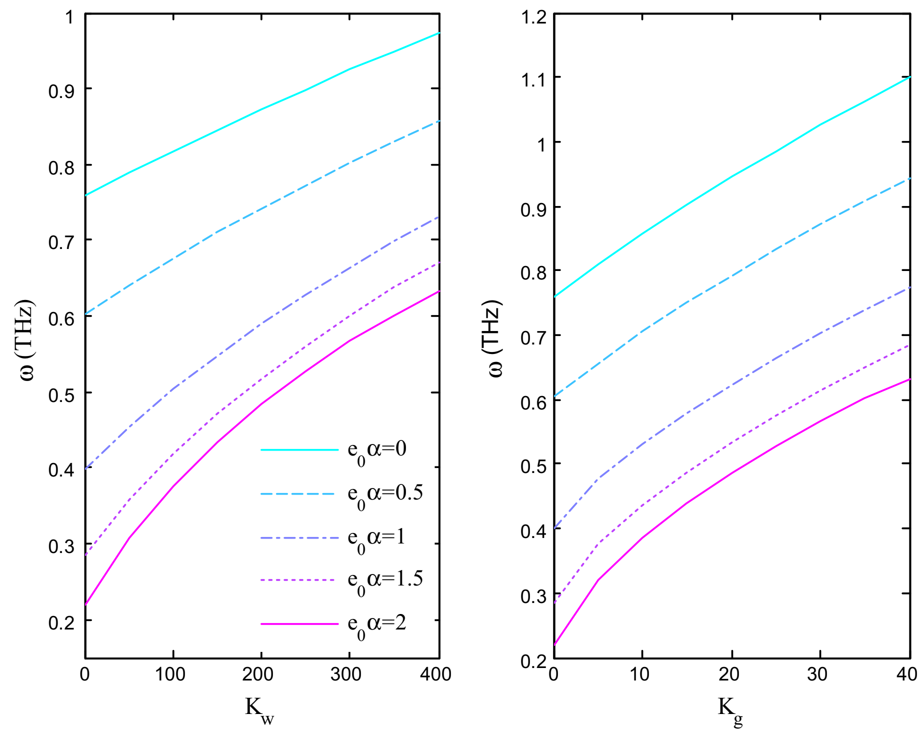

Fig. 4 Fundamental frequencies of simply supported CNC versus Winkler and Pasternak coefficients of elastic foundation $\left(\frac{R_1}{h}=4,\ 2\beta=60, \frac{L}{R_1}=2\right)$

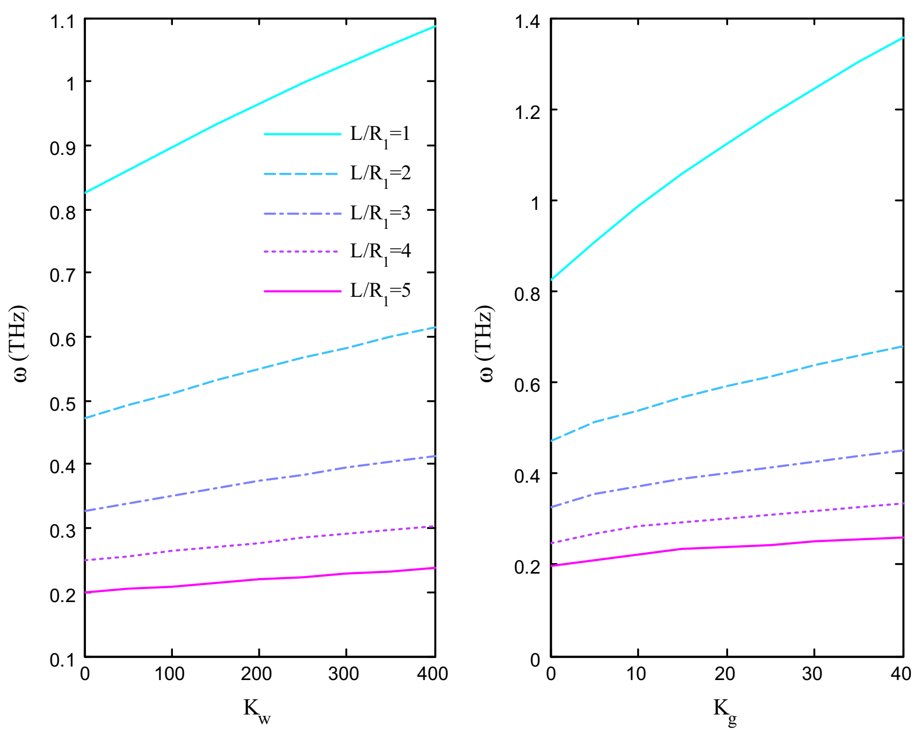

Fig. 5 Fundamental frequencies of simply supported CNC versus Winkler and Pasternak coefficients of elastic foundation $\left(\frac{R_1}{h}=5, 2\beta=60,\ e_0\alpha=0.5\ \mathrm{nm}\right)$

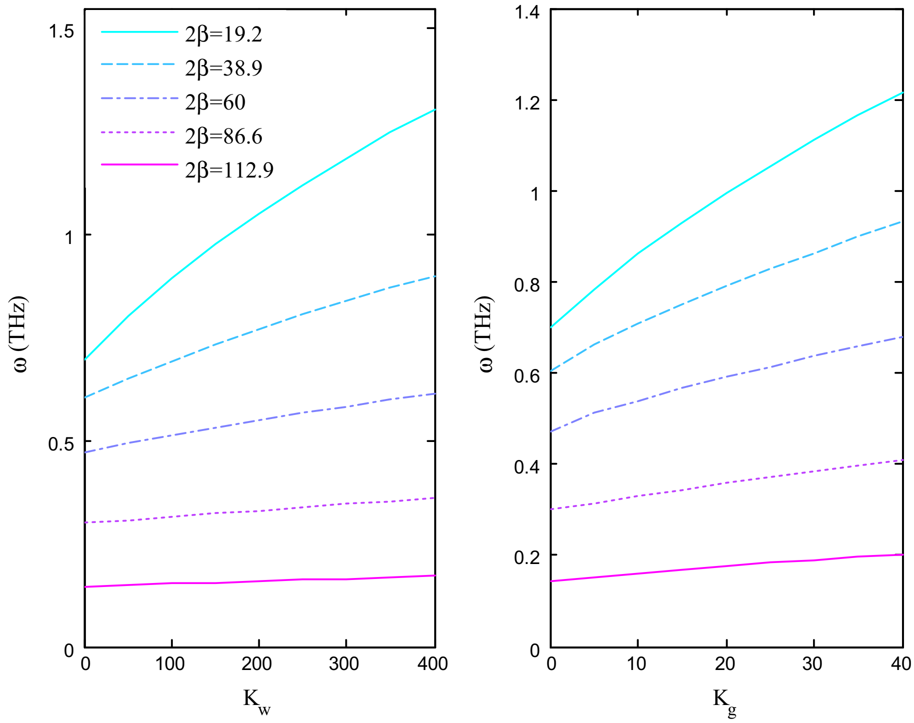

Fig. 6 Fundamental frequencies of simply supported CNC versus Winkler and Pasternak coefficients of elastic foundation $\left(\frac{R_1}{h} = 5,\ \frac{L}{R_1} = 2,\ e_0\alpha = 0.5\ \text{nm}\right)$

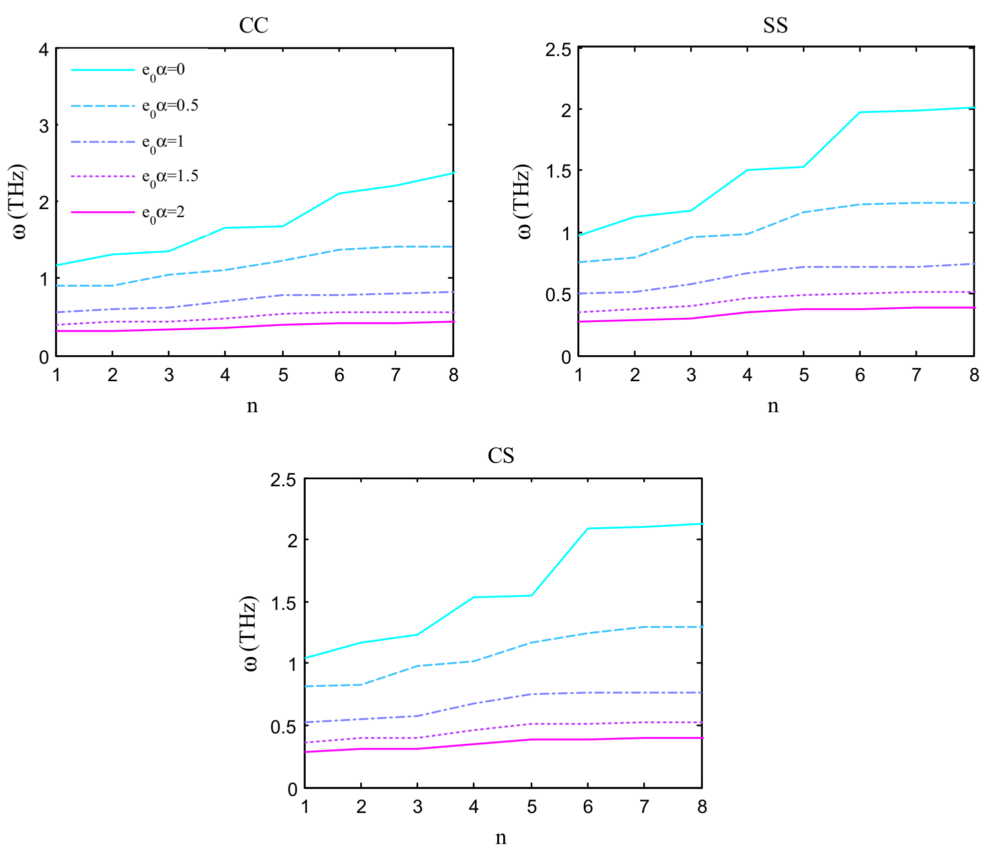

Fig. 7 Natural frequencies of CNC versus mode numbers $\left(\frac{R_1}{h} = 4,\ 2\beta = 38.9,\ \frac{L}{R_1} = 2,\ K_w = 0,\ K_g = 0\right)$

Table 2 Fundamental frequencies (THz) of embedded CNC for various nonlocal parameters and boundary conditions $\left(\frac{R_1}{h} = 5,\ 2\beta = 38.9,\ \frac{L}{R_1} = 3\right)$

K_w	K_g	$e_0\alpha = 0\,(\mathrm{nm})$			$e_0\alpha = 0.5\,(\mathrm{nm})$			$e_0\alpha = 1\,(\mathrm{nm})$		
		CC	SS	CS	CC	SS	CS	CC	SS	CS
0	0	0.535	0.484	0.502	0.474	0.433	0.444	0.340	0.315	0.321
	10	0.590	0.542	0.559	0.535	0.492	0.507	0.440	0.404	0.417
	20	0.640	0.595	0.610	0.587	0.544	0.559	0.495	0.458	0.470
100	0	0.581	0.535	0.551	0.527	0.489	0.502	0.413	0.392	0.397
	10	0.632	0.588	0.603	0.581	0.541	0.555	0.495	0.463	0.474
	20	0.679	0.636	0.651	0.629	0.589	0.603	0.543	0.510	0.521
200	0	0.623	0.581	0.596	0.573	0.539	0.552	0.474	0.456	0.461
	10	0.671	0.630	0.644	0.623	0.587	0.600	0.543	0.515	0.525
	20	0.715	0.675	0.689	0.668	0.631	0.644	0.588	0.557	0.568

and results indicated that the increase in Winkler and Pasternak coefficients makes the structure stiffer and increases the natural frequencies. Also, the presence of elastic medium results in reduction of nonlocal effect and the cone with the smaller apex angels is more affected by elastic foundation coefficients. Additionally, the higher mode numbers of natural frequency of CNCs are more size dependent.

References

1. M. Ge, K. Sattler, Observation of Fullerene Cones. Chem. Phys. Lett. **220**, 192–196 (1994)
2. A. Krishnan, E. Dujardin, M.M.J. Treacy, J. Hugdahl, S. Lynum, T.W. Ebbesen, Graphitic cones and the nucleation of curved carbon surfaces. Nature **388**, 451–454 (1997)
3. A. Mohammadi, F. Kaminski, V. Sandoghdar, M. Agio, Fluorescence enhancement with the optical (bi-) conical antenna. J. Phys. Chem. C **114**, 7372–7377 (2010)
4. C. Yeh, M. Chen, J. Hwang, J.Y. Gan, C. Kou, Field emission from a composite structure consisting of vertically aligned single-walled carbon nanotubes and carbon nanocones. Nanotechnology **17**, 5930–5934 (2006)
5. S. Akita, M. Nishio, Y. Nakayama, Buckling of multiwall carbon nanotubes under axial compression. Jpn. J. Appl. Phys. **45**, 5586–5589 (2006)
6. Y.R. Jeng, P.C. Tsai, T.H. Fang, Experimental and numerical investigation into buckling instability of carbon nanotube probes under nanoindentation. Appl. Phys. Lett. **90**, 161913 (2007)
7. M. Endo, Y.A. Kim, T. Hayashi, Y. Fukai, K. Oshida, M. Terrones, T. Yanagisawa, S. Higaki, M.S. Dresselhaus, Structural characterization of cup-stacked-type nanofibers with an entirely hollow core. Appl. Phys. Lett. **80**, 1267 (2002)
8. H. Terrones, T. Hayashi, M. Muñoz-Navia, M. Terrones, Y.A. Kim, N. Grobert, R. Kamalakaran, J. Dorantes-Dávila, R. Escudero, M.S. Dresselhaus, M. Endo, Graphitic cones in palladium catalysed carbon nanofibres. Chem. Phys. Lett. **343**, 241 (2001)
9. M.M.S. Fakhrabadi, N. Khani, S. Pedrammehr, Vibrational analysis of single-walled carbon nanocones using molecular mechanics approach. Phys. E **44**, 1162–1168 (2012)
10. Y.G. Hu, K.M. Liew, X.Q. He, Z. Li, J. Han, Free transverse vibration of single-walled carbon nanocones. Carbon **50**, 4418–4423 (2012)
11. R.D. Firouz-Abadi, H. Amini, A.R. Hosseinian, Assessment of the resonance frequency of cantilever carbon nanocones using molecular dynamics simulation. Appl. Phys. Lett. **100**, 173108 (2012)
12. P. Tsai, T. Fang, A molecular dynamics study of the nucleation, thermal stability and nanomechanics of carbon nanocones. Nanotechnology **18**, 105702 (2007)
13. R. Ansari, A. Momen, S. Rouhi, S. Ajori, On the vibration of single-walled carbon nanocones: molecular mechanics approach versus molecular dynamics simulations. Shock Vib. **2014**, 410783 (2014)
14. T. Belytschko, S.P. Xiao, G.C. Schatz, R.S. Ruoff, Atomistic simulations of nanotube fracture. Phys. Rev. B **65**, 235430 (2002)
15. J.W. Yan, L.W. Zhang, K.M. Liew, L.H. He, A higher-order gradient theory for modeling of the vibration behavior of single-wall carbon nanocones. Appl. Math. Model. **38**, 2946–2960 (2014)
16. P. Sharma, S. Ganti, N. Bhate, Effect of surfaces on the size-dependent elastic state of nano-inhomogeneities. Appl. Phys. Lett. **82**, 535 (2003)
17. C.T. Sun, H. Zhang, Size-dependent elastic moduli of plate like nanomaterials. J. Appl. Phys. **93**, 1212 (2003)
18. A.C. Eringen, On differential equations of nonlocal elasticity and solutions of screw dislocation and surface waves. J. Appl. Phys. **54**, 4703–4710 (1983)
19. A.C. Eringen, *Nonlocal Continuum Field Theories* (Springer, New York, 2002)
20. J. Peddieson, G.R. Buchanan, R.P. McNitt, Application of nonlocal continuum models to nanotechnology. Int. J. Eng. Sci. **41**, 305–312 (2003)
21. B. Arash, Q. Wang, Vibration of single- and double-layered graphene sheets. J. Nanotechnol. Eng. Med. **2**, 011012 (2011)
22. M. Mohammadi, M. Ghayour, A. Farajpour, Free transverse vibration analysis of circular and annular graphene sheets with various boundary conditions using the nonlocal continuum plate model. Compos.: Part B **45**, 32–42 (2013)
23. Y.Q. Zhang, G.R. Liu, J.S. Wang, Small-scale effects on buckling of multiwalled carbon nanotubes under axial compression. Phys. Rev. B **70**, 205430 (2004)
24. Q. Wang, V.K. Varadan, S.T. Quek, Small scale effect on elastic buckling of carbon nanotubes with nonlocal continuum models. Phys. Lett. A **357**, 130–135 (2006)
25. S.C. Pradhan, G.K. Reddy, Analysis of single walled carbon nanotube on Winkler foundation using nonlocal elasticity theory and DTM. Comput. Mater. Sci. **50**, 1052–1056 (2011)
26. R. Ansari, J. Torabi, Nonlocal vibration analysis of circular double-layered graphene sheets resting on elastic foundation

subjected to thermal loading. Acta. Mech. Sin. **32**, 841–853 (2016)

27. R.F. Gibson, O.E. Ayorinde, Y.F. Wen, Vibration of carbon nanotubes and their composites: a review. Compos. Sci. Technol. **67**, 1–28 (2007)
28. A.R. Setoodeh, M. Khosrownejad, P. Malekzadeh, Exact nonlocal solution for postbuckling of single-walled carbon nanotubes. Phys. E **43**, 1730–1737 (2011)
29. H.S. Shen, C.L. Zhang, Nonlocal beam model for nonlinear analysis of carbon nanotubes on elastomeric substrates. Comput. Mater. Sci. **50**, 1022–1029 (2011)
30. L. Ke, Y. Xiang, J. Yang, S. Kitipornchai, Nonlinear free vibration of embedded double-walled carbon nanotubes based on nonlocal Timoshenko beam theory. Comput. Mater. Sci. **47**, 676–683 (2009)
31. T. Murrmu, S.C. Pradhan, Thermo-mechanical vibration of a single-walled carbon nanotube embedded in an elastic medium based on nonlocal elasticity theory. Comput. Mater. Sci. **46**, 854–859 (2009)
32. R. Ansari, H. Ramezannezhad, Nonlocal Timoshenko beam model for the large-amplitude vibrations of embedded multi-walled carbon nanotubes including thermal effects. Phys. E **43**, 1171–1178 (2011)
33. R. Ansari, A. Shahabodini, H. Rouhi, A thickness-independent nonlocal shell model for describing the stability behavior of carbon nanotubes under compression. Compos. Struct. **100**, 323–331 (2013)
34. R. Li, G.A. Kardomateas, Vibration characteristics of multi-walled carbon nanotubes embedded in elastic media by a nonlocal elastic shell model. J. Appl. Mech. **74**, 1087–1094 (2007)
35. R. Ansari, H. Rouhi, Analytical treatment of the free vibration of single-walled carbon nanotubes based on the nonlocal Flugge shell theory. ASME J. Eng. Mater. Technol. **134**, 011008 (2012)
36. M.J. Hao, X.M. Guo, Q. Wang, Small-scale effect on torsional buckling of multi-walled carbon nanotubes. Eur. J. Mech. A. Solids **29**, 49–55 (2010)
37. Y.G. Hu, K.M. Liew, Q. Wang, X.Q. He, B.I. Yakobson, Nonlocal shell model for elastic wave propagation in single- and double-walled carbon nanotubes. J. Mech. Phys. Solids **56**, 3475–3485 (2008)
38. R. Ansari, H. Rouhi, S. Sahmani, Calibration of the analytical nonlocal shell model for vibrations of double-walled carbon nanotubes with arbitrary boundary conditions using molecular dynamics. Int. J. Mech. Sci. **53**, 786–792 (2011)
39. Q.G. Shu, P.Y. Shau, Axial vibration analysis of nanocones based on nonlocal elasticity theory. Acta. Mech. Sin. **28**, 801–807 (2012)
40. T.P. Chang, Small scale effect on axial vibration of nonuniform and non-homogeneous nanorods. Comput. Mater. Sci. **54**, 23–27 (2012)
41. R. Firouz-Abadi, M. Fotouhi, H. Haddadpour, Free vibration analysis of nanocones using a nonlocal continuum model. Phys. Lett., Sect. A: Gen., At. Solid State Phys. **375**, 3593–3598 (2011)
42. R. Firouz-Abadi, M. Fotouhi, H. Haddadpour, Stability analysis of nanocones under external pressure and axial compression using a nonlocal shell model. Phys. E **44**, 1832–1837 (2012)
43. M.M. Fotouhi, R.D. Firouz-Abadi, H. Haddadpour, Free vibration analysis of nanocones embedded in an elastic medium using a nonlocal continuum shell model. Int. J. Eng. Sci. **64**, 14–22 (2013)
44. R. Ansari, H. Rouhi, A.N. Rad, Vibrational analysis of carbon nanocones under different boundary conditions: an analytical approach. Mech. Res. Commun. **56**, 130–135 (2014)
45. J. Fernández-Sáez, R. Zaera, J.A. Loya, J.N. Reddy, Bending of Euler–Bernoulli beams using Eringen's integral formulation: a paradox resolved. Int. J. Eng. Sci. **99**, 107–116 (2016)
46. M. Tuna, M. Kirca, Exact solution of Eringen's nonlocal integral model for bending of Euler–Bernoulli and Timoshenko beams. Int. J. Eng. Sci. **105**, 80–92 (2016)
47. R. Ansari, J. Torabi, M.F. Shojaei, Vibrational analysis of functionally graded carbon nanotube-reinforced composite spherical shells resting on elastic foundation using the variational differential quadrature method. Eur. J. Mech.-A/Solids **60**, 166–182 (2016)
48. R. Ansari, J. Torabi, M.F. Shojaei, E. Hasrati, Buckling analysis of axially-loaded functionally graded carbon nanotube-reinforced composite conical panels using a novel numerical variational method. Compos. Struct. **157**, 398–411 (2016)
49. R. Ansari, J. Torabi, M.F. Shojaei, Buckling and vibration analysis of embedded functionally graded carbon nanotube-reinforced composite annular sector plates under thermal loading. Compos. Part B: Eng. **109**, 197–213 (2016)
50. C. Shu, *Differential Quadrature and its Application in Engineering* (Springer, London, 2000)
51. F. Tornabene, E. Viola, D.J. Inman, 2-D differential quadrature solution for vibration analysis of functionally graded conical, cylindrical shell and annular plate structures. J. Sound Vib. **328**, 259–290 (2009)
52. R. Ansari, V. Mohammadi, M. Faghih Shojaei, R. Gholami, H. Rouhi, Nonlinear vibration analysis of Timoshenko nanobeams based on surface stress elasticity theory. Eur. J. Mech. A/Solids **45**, 143–152 (2014)
53. C.Y. Wei, D. Srivastava, Nanomechanics of carbon nanofibers: structural and elastic properties. Appl. Phys. Lett. **85**, 2208–2210 (2004)
54. J.X. Wei, K.M. Liew, X.Q. He, Mechanical properties of carbon nanocones. Appl. Phys. Lett. **91**, 261906 (2007)